The Journal of Experimental Biology 214, 1153-1162

doi:10.1242/jeb.046045

RESEARCH ARTICLE

Hydrodynamic stability of the painted turtle (*Chrysemys picta*): effects of four-limbed rowing *versus* forelimb flapping in rigid-bodied tetrapods

Gabriel Rivera*,†, Angela R. V. Rivera and Richard W. Blob

Department of Biological Sciences, Clemson University, 132 Long Hall, Clemson, SC 29634, USA

*Present address: Department of Ecology, Evolution and Organismal Biology, Iowa State University, Ames, IA 50011, USA
†Author for correspondence (grivera@iastate.edu)

Accepted 3 December 2010

SUMMARY

Hydrodynamic stability is the ability to resist recoil motions of the body produced by destabilizing forces. Previous studies have suggested that recoil motions can decrease locomotor performance, efficiency and sensory perception and that swimming animals might utilize kinematic strategies or possess morphological adaptations that reduce recoil motions and produce more stable trajectories. We used high-speed video to assess hydrodynamic stability during rectilinear swimming in the freshwater painted turtle (*Chrysemys picta*). Parameters of vertical stability (heave and pitch) were non-cyclic and variable, whereas measures of lateral stability (sideslip and yaw) showed repeatable cyclic patterns. In addition, because freshwater and marine turtles use different swimming styles, we tested the effects of propulsive mode on hydrodynamic stability during rectilinear swimming, by comparing our data from painted turtles with previously collected data from two species of marine turtle (*Caretta caretta* and *Chelonia mydas*). Painted turtles had higher levels of stability than both species of marine turtle for six of the eight parameters tested, highlighting potential disadvantages associated with 'aquatic flight'. Finally, available data on hydrodynamic stability of other rigid-bodied vertebrates indicate that turtles are less stable than boxfish and pufferfish.

Key words: biomechanics, locomotion, swimming, performance, hydrodynamics, stability, turtle.

INTRODUCTION

Swimming animals are subjected to a variety of potentially destabilizing forces that can be either self-generated (e.g. propulsor movements) or external (e.g. environmental turbulence). These forces produce recoil motions that have both rotational (pitch, yaw, and roll) and translational (heave, sideslip and surge) components (Hove et al., 2001). Hydrodynamic stability is the ability to resist recoil motions of the body produced by destabilizing forces and correct for self-generated and external disturbances, including recoil motions produced during swimming, thereby allowing maintenance of a given trajectory (Bartol et al., 2003; Webb, 2002; Weihs, 2002). Previous studies have suggested that destabilizing recoil motions can decrease locomotor performance and efficiency as a result of increased drag and laterally directed thrust, and inhibit sensory perception as a result of extraneous motion of the head (Bainbridge, 1963; Lighthill, 1975; Lighthill, 1977; Webb, 1992; Webb, 2002; Weihs, 2002). These observations suggest that swimming animals might utilize kinematic strategies [e.g. corrective forelimb and hindlimb motions in sea turtles (see Avens et al., 2003)] or possess morphological adaptations [e.g. carapacial keels in boxfishes (see Bartol et al., 2003)] that damp destabilizing forces, reducing recoil motions and producing more stable trajectories.

Although hydrodynamic stability has been assessed for a phylogenetically diverse array of vertebrate taxa, the effects of many different body designs and modes of propulsion remain unknown. For example, among rigid-bodied taxa, few data on stability are available for animals propelled by jointed appendages (e.g. limbed tetrapods). Turtles provide an ideal system in which to evaluate effects of propulsion using oscillatory motions of jointed appendages on stability. In turtles, the vertebrae are fused dorsally with a bony carapace, precluding movement of the axial skeleton between the base of the neck and the tail. As a result of their immobilized axial skeleton and reduced tail, thrust in swimming turtles is generated exclusively by the movements of forelimbs and hindlimbs (Blob et al., 2008; Pace et al., 2001). Marine and freshwater turtle species have evolved different limb morphologies and corresponding modes of propulsion (Davenport et al., 1984). In marine turtles (seven species) the forelimbs are modified into flat, elongate flippers and the hindlimbs are reduced in size. In contrast, freshwater turtles (over 100 species) have distinct forelimb and hindlimb segments with webbed forefeet and hindfeet and have more similarly sized forelimbs and hindlimbs (Pace et al., 2001). Marine turtles are capable of using several swimming modes, but post-hatchling turtles generate thrust predominantly *via* synchronous dorsoventral movements of their forelimbs, a propulsive mode referred to as aquatic flight, which presumably involves lift-based propulsive forces (Wyneken, 1997) (Fig. 1A). In contrast, nearly all freshwater species propel themselves *via* synchronous, anteroposterior rowing movements of contralateral forelimbs and hindlimbs (Davenport et al., 1984; Renous et al., 2008; Rivera et al., 2006). In this mode of locomotion, in contrast to aquatic flight, the two contralateral forelimb–hindlimb sets move asynchronously, producing drag-based thrust. Thus, during typical steady swimming, freshwater turtles propel themselves using all four limbs, whereas non-hatchling sea turtles predominantly use their two foreflippers, with the hindflippers serving mainly as rudders (Fig. 1A,B).

Although a number of studies have examined aspects of swimming in aquatic turtles, including kinematics (Davenport et al., 1984; Pace et al., 2001; Renous et al., 2008; Zug, 1971), motor control (Blob et al., 2008; Gillis and Blob, 2001; Rivera and Blob,

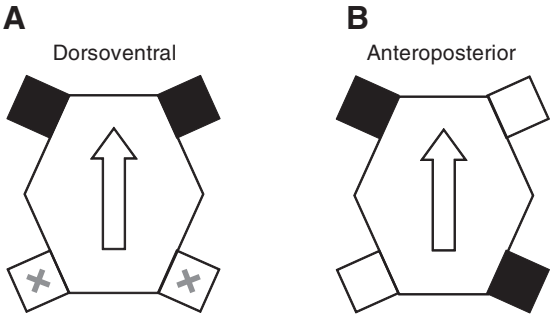

Fig. 1. Diagram of locomotor modes used by (A) marine turtles and (B) freshwater turtles. Limbs of the same color move in-phase, while those of opposite colors move in anti-phase (*sensu* Long et al., 2006). 'Dorsoventral' and 'anteroposterior' describe the primary direction of motion for the limbs. During synchronous dorsoventral flapping [as collected in Dougherty et al. (Dougherty et al., 2010)], limbs marked 'X' lack propulsive function. Arrows point anteriorly.

2010), maneuverability (Heithaus et al., 2002; Rivera et al., 2006) and hydrodynamic implications of shell morphology (Aresco and Dobie, 2000; Claude et al., 2003; Lubcke and Wilson, 2007; Rivera, 2008; Rivera and Claude, 2008), relatively little is known about hydrodynamic stability in this lineage. Dougherty et al. examined stability in post-hatchlings of two species of marine turtles [*Caretta caretta* (Linnaeus 1758) and *Chelonia mydas* (Linnaeus 1758)], providing a quantitative description of recoil motions throughout the limb cycle during rectilinear swimming using synchronous flapping (i.e. dorsoventral) propulsion (Dougherty et al., 2010). However, despite the greater diversity of freshwater turtles and their use of rowing (i.e. anteroposterior) propulsive movements that are probably basal for the entire lineage (Joyce and Gauthier, 2004), no study has yet examined hydrodynamic stability in these taxa.

Given the differences in typical modes of propulsion used by freshwater and post-hatchling marine turtles, several testable hypotheses can be generated for how hydrodynamic stability might differ between these groups. (1) The primary direction of motion for propulsors during the dominant swimming modes (i.e. contralateral rowing in freshwater turtles and synchronous foreflipper flapping in sea turtles) is anteroposterior in freshwater turtles and dorsoventral in post-hatchling marine turtles. Because freshwater turtles move their limbs in the same plane as their direction of travel, we predict that heave will be lower in freshwater turtles. (2) Freshwater turtles produce thrust by oscillating all four limbs during swimming, whereas post-hatchling marine turtles produce thrust primarily with motions of their forelimbs. Because marine turtles predominantly oscillate limbs at one end of the body (anterior) in dorsoventral motions, we predict that pitch will be higher in marine turtles. (3) Motions of homologous limbs on the left and right side are asynchronous in freshwater turtles and synchronous in marine turtles during their primary swimming modes. Because mirrored motions occur at the same time on both sides of the body in marine turtles, we predict that freshwater turtles will have higher levels of lateral recoil (sideslip and yaw).

As a result of the differences in propulsive limb movements between freshwater and post-hatchling marine turtles during rectilinear swimming, and because freshwater turtles possess a body design that differs strongly from that of other rigid-bodied species in which stability has been examined (i.e. boxfish and pufferfish), freshwater turtles provide an important comparison for evaluating the effects of limb kinematics and morphological design on hydrodynamic stability in vertebrates. Furthermore, a comparison of measures of stability between freshwater and marine turtles may provide insights into the evolution of the two different styles of propulsion seen in extant turtles. The goals of this study were, therefore, to: (1) quantify hydrodynamic stability of the body and head in swimming freshwater turtles, and (2) test the effects of different modes of propulsion on stability among turtles by comparing our data with a previous study of sea turtle species using similar methods (Dougherty et al., 2010).

MATERIALS AND METHODS

Animals

Stability data were collected from four juvenile painted turtles [*Chrysemys picta* (Schneider 1783); carapace length: 9.6–11.6 cm]. Turtles were obtained from a commercial turtle supplier and housed together in a climate-controlled greenhouse exposed to ambient light. All animal care and experimental procedures followed Clemson University IACUC guidelines (Clemson University AUP #2007-069).

Experiments

Each turtle was placed individually into a glass aquarium (152×61×64 cm) filled with water (28–30°C) to a depth of 26 cm. The tank was fitted with a manually powered top-mounted sliding rail system that spanned its entire length, was centered between the front and back walls, and supported a vertical sting that descended into the water. Turtles were stimulated to swim in a straight line by luring them with a prey stimulus (earthworm) that was attached to the base of the vertical sting, which was submerged 8 cm below the surface of the water. Use of the rail system ensured that the prey stimulus traversed the tank with no lateral or vertical displacement and, thus, minimized intentional lateral and vertical movements of the pursuing turtle. For each individual, all trials were collected within the span of 1 week. This experimental design was similar to that used in Dougherty et al. and facilitated comparisons with marine turtles from that study (Dougherty et al., 2010).

Linear swimming trials were filmed simultaneously at 100 Hz in lateral and ventral views using two digitally synchronized high-speed video cameras (Phantom V5.1, Vision Research, Inc., Wayne, NJ, USA). The lateral view provided information on vertical stability and the ventral view provided information on lateral stability. The ventral view was captured using a mirror placed at a 45 deg angle to the tank bottom. Both cameras were focused on the central, approximately 100 cm, segment of the test tank. Each filming view included a 1 cm square grid used to provide distance calibration for video analyses.

Measurement of stability and limb kinematics

Each set of video files was cropped to include the straightest swimming trajectory over three consecutive limb cycles. A limb cycle was defined as the period beginning at maximum retraction of the left forelimb and ending on the subsequent maximum retraction of the left forelimb. The positions of landmarks on the head, shell and limbs were then digitized in lateral view (three landmarks: tip of snout, anterior edge of carapace, posterior edge of carapace; Fig. 2A) and ventral view (11 landmarks: tip of snout, anterior and posterior edge of plastron, left and right shoulder, left and right elbow, left and right hip, left and right knee; Fig. 2B) using DLTdataviewer2 software (Hedrick, 2008).

Digitized coordinate data were input into a custom Matlab (ver. 7.1, Mathworks, Inc., Natick, MA, USA) routine that interpolated 98 equidistant points between the anterior and posterior points on the carapace (lateral view) and plastron (ventral view), yielding 100

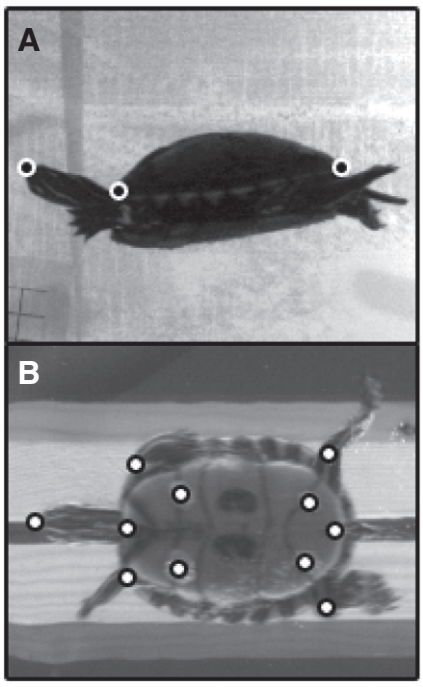

Fig. 2. Points that were digitized on painted turtles in (A) lateral and (B) ventral views. See text for landmark descriptions.

equidistant points along the respective body axis. For each view, the point along the body axis with the most stable trajectory throughout the trial (i.e. the point that traveled the smallest cumulative distance) was designated as the center of rotation (COR) (Dougherty et al., 2010; Rivera et al., 2006; Walker, 2000). Linear regressions were calculated using the *x*- and *y*-coordinates of the COR from each frame of the trial and the resulting R^2-values provided a measure of linearity of the swimming path. In addition, the horizontal distance traveled for each swimming trial (in body lengths; BL) was calculated as the cumulative displacement of the COR in ventral view. Linear velocity (in BL s^{-1}) was calculated from differentiation of the cumulative displacement of the COR along the swimming path (based on the *x* and *y* positional data). Data were smoothed using a quintic spline [generalized cross validation (see Walker, 1998)] and then differentiated using a custom Matlab routine.

Because calculations of all stability variables (see below) were based on the linear equations of the swimming path, only trials meeting the following criteria were used. (1) $R^2>0.25$ for both lateral and ventral views to ensure linear swimming. Some previous studies using similar techniques used much larger R^2-values [>0.9 (Wassersug and von Seckendorf Hoff, 1985)]; however, it is possible that such strict cut-off values would bias results to appear more stable than is representative (Dougherty et al., 2010). (2) Turtles traveled a minimum horizontal distance of three body lengths. (3) Turtles completed a minimum of three consecutive limb cycles during steady swimming (i.e. not starting or stopping) in the field of view of the camera. Trials that met these criteria were subdivided into individual limb cycles, for which values for distance and velocity, limb kinematics and stability were calculated.

To evaluate the kinematic patterns that turtles used during limb cycles, a Matlab routine was used to calculate the movements of each of the four limbs relative to the midline axis of the body throughout each limb cycle. Angles were calculated from the ventral view videos as two-dimensional projections onto the horizontal plane, with a limb segment parallel to the midline axis with the distal end oriented cranially assigned an angle of 0 deg, whereas one parallel to the midline with the distal end oriented caudally assigned an angle of 180 deg. A quintic spline was fitted to the kinematic calculations from each limb cycle, smoothing the data and allowing cycles to be normalized to the same duration (101 equally spaced increments representing 0–100% of limb cycle) prior to comparisons. These values were used to produce mean (±s.e.m.) profiles of limb kinematics (Pace et al., 2001).

To evaluate stability during limb cycles a Matlab routine was used to rotate and translate all digitized coordinates for each view so that the swimming path associated with each limb cycle (as previously calculated from trial data) was defined by a vector starting at the origin and traveling along the positive *x*-axis. All stability variables (i.e. heave, pitch, sideslip, yaw) were then derived from the relationship between the swimming path (i.e. positive *x*-axis) and three additional parameters calculated from the reconfigured coordinates: (1) the position of the COR throughout the limb cycle; (2) the position and orientation of the head throughout the limb cycle, which was calculated from the line segment formed between the tip of the snout and the anterior points of the carapace (lateral) and plastron (ventral); and (3) the position and orientation of the body axis throughout the limb cycle, which was calculated from the line segment formed between the anterior and posterior points of the carapace (lateral) and plastron (ventral). As with the kinematic data, a quintic spline was fitted to stability calculations from each limb cycle, smoothing the data and allowing the limb cycles to be normalized to the same duration prior to comparisons. These values were used to quantify stability variables (see below), produce mean (±s.e.m.) profiles of stability parameters throughout the limb cycle, and allowed patterns of stability to be related to the motion of the limbs throughout the limb cycle. The available camera setup did not allow for collection of surge [because of the difficulties of calculating accelerations from digitized videos (see Walker, 1998)] or roll (because of the orientation of the two cameras required to acquire data for heave, pitch, sideslip and yaw).

To quantify specific stability variables (Table 1), the maximum angular and positional displacements were extracted from the smoothed and normalized data of each limb cycle. Maximum angular displacements (pitch or yaw) were defined as the maximum angle between the path of travel and the corresponding body axis. Maximum positional displacements (heave and sideslip) were defined by the orthogonal distance between the COR and the path of travel and were calculated as proportions of body (=carapace) length. Excursion values were calculated as the difference between the maximum and minimum values for each stability parameter. Owing to the bilaterally symmetrical nature of the study system, in the case of yaw and sideslip, the single (left or right side) maximum value was extracted; excursion values for yaw and sideslip were calculated as the difference between the maximum left and right deviations. In addition, because the maximum value for a given trial does not always occur at the same percent of the limb cycle, it is also possible that calculated maximum values may be different from the maximum values seen in mean kinematic profiles (Dougherty et al., 2010).

In addition to stability measures, the distance traveled for each limb cycle (i.e. stride length) was calculated as the cumulative displacement of the COR during the limb cycle. Additionally, linear velocity was calculated from differentiation of the cumulative displacement of the COR along the swimming path. Distance and velocity were calculated from ventral view data and were smoothed and normalized as previously described for the kinematic and stability data.

Table 1. Stability parameters collected from individual limb cycles

Stability parameters	Definition
Body	
Maximum heave magnitude*,‡	Maximum vertical distance of COR from path of travel
Maximum positive heave*	Maximum distance of COR above path of travel
Maximum negative heave*	Maximum distance of COR below path of travel
Heave excursion*,‡	Distance between maximum positive and negative heave values
Maximum pitch magnitude*,‡	Maximum angle of body axis from path of travel
Maximum positive pitch*	Maximum positive angle of body axis from path of travel
Maximum negative pitch*	Maximum negative angle of body axis from path of travel
Pitch excursion*,‡	Angle between maximum positive and negative pitch values
Maximum sideslip magnitude†,‡	Maximum lateral distance of COR from path of travel
Sideslip excursion†,‡	Distance between maximum left and maximum right sideslip values
Maximum yaw magnitude †,‡	Maximum lateral angle of body axis from path of travel
Yaw excursion†,‡	Angle between maximum left and right yaw values
Head	
Vertical head/body angle magnitude*	Maximum vertical angle of head axis relative to body axis
Vertical head/body angle excursion*	Angle between maximum and minimum vertical head/body angles
Lateral head/body angle magnitude†	Maximum lateral angle of head axis relative to body axis
Lateral head/body angle excursion†	Angle between maximum and minimum vertical head/body angles
Maximum head yaw magnitude †	Maximum lateral angle of head axis from the path of travel
Maximum head yaw excursion†	Angle between maximum left and right head yaw values
Maximum nose displacement†	Maximum lateral distance of nose from path of travel

Values for heave, sideslip and maximum nose displacement are calculated in body lengths (BL).
Values for pitch and yaw are calculated in degrees.
All distances are measured orthogonal to the path of travel.
*Variables calculated from lateral view videos and refer to vertical displacements and angles.
†Variables calculated from ventral view videos and refer to lateral displacements and angles.
‡Focal parameters used in interspecific comparisons.

Statistical analysis

Prior to analysis, outliers (values greater than three standard deviations from the mean) were removed from the data set. Because ANOVA designs (see below) required three cycles from each trial, any trial containing a cycle with an outlier was excluded from the data set. Data were transformed as needed to meet assumptions of homoscedasticity and normality (Sokal and Rohlf, 1995). ANOVA was used to conduct separate intraspecific and interspecific comparisons. For intraspecific comparisons, a set of nested ANOVAs (individual>trial) was used to test for individual differences between the four painted turtles for the 12 measured stability parameters. For these analyses, 'individual' was analyzed as a fixed factor and 'trial' (nested within individual) was treated as a random factor. For interspecific comparisons, a set of multi-level nested ANOVAs (species>individual>trial) was applied to compare data for eight focal stability parameters (see Table 1) between freshwater turtles (this study) and two species of marine turtles (Dougherty et al., 2010). 'Species' was analyzed as a fixed factor, and the remaining two levels, 'individual' (nested within species) and 'trial' (nested within individual × species), were treated as random factors. Pair-wise nested ANOVAs were used to identify differences between individual species. Sequential Bonferroni corrections (Holm, 1979; Rice, 1989) were applied to all intraspecific, interspecific and pair-wise comparisons. Additionally, correlation and regression analyses were used to examine the relationships between path of travel linearity (i.e. R^2-values), limb motions, swimming velocity and stability parameters. In contrast to ANOVAs, these analyses required that cycles be treated as an independent data points, leading to an inflation of the degrees of freedom. Nevertheless, these analyses are used to demonstrate general relationships and patterns within the data, rather than to test the significance of specific hypotheses. Nested ANOVAs were performed using SYSTAT 12 (Systat Software, Inc., Chicago, IL, USA); correlations and regressions were performed using SPSS Base (v. 10; SPSS, Inc., Chicago, IL, USA).

RESULTS

Data were analyzed for 32 trials (6–11 per turtle), yielding 96 limb cycles for which stability parameters were measured. Horizontal body displacement during trials ranged from 3.2 to 5.9 BL (4.0±0.1; mean ± s.e.m., N=32 for this and subsequent values unless stated otherwise), with mean swimming velocities between 2.7 and 5.5 BL s^{-1} (3.9±0.1). The mean anatomical position of the COR during trials was 26.0±4.6% of carapace length and 38.1±2.0% of plastron length, based on lateral and ventral views, respectively. The R^2-values from regressions used to determine the path of travel ranged from 0.30 to 0.97 (0.67±0.03) for lateral stability parameters (sideslip and yaw) and from 0.26 to 0.99 (0.75±0.03) for vertical parameters (heave and pitch). The correlation between lateral and ventral R^2-values (i.e. linearity of path of travel) was not significant (Pearson correlation, r=0.007, P=0.969, N=32), indicating that lateral and ventral stability parameters are controlled independently from each other. The linearity of the lateral and ventral path of travel, however, were significantly correlated with several body stability parameters (Table 2).

Horizontal body displacement during individual cycles (i.e. stride length) ranged from 1.0 to 2.2 BL (1.3±0.02, N=96). Mean swimming velocities for each cycle ranged between 2.6 and 5.6 BL s^{-1} (3.9±0.1, N=96). Swimming velocity had no significant effect on stride length across observed speeds (R^2=0.003, P=0.610, N=96).

Limb kinematics

During rectilinear swimming, painted turtles use synchronous movements of contralateral forelimbs and hindlimbs (Fig. 3). The angle between the forelimbs and body axis ranged from –23.0 to 92.3 deg, and the angle between the hindlimbs and body axis ranged from 46.6 to 165.1 deg. By definition, maximum retraction of the left forelimb always occurs at 0% of the limb cycle. Based on how a limb cycle is defined, the switch from retraction (power stroke)

Table 2. Pearson correlations (r) between path linearity (R^2 of path of travel) and stability parameters in painted turtles

Stability parameters	r
Maximum heave magnitude†	**–0.357***
Maximum positive heave†	**–0.265**
Maximum negative heave†	0.162
Heave excursion†	**–0.281**
Maximum pitch magnitude†	**–0.269**
Maximum positive pitch†	**–0.210**
Maximum negative pitch†	–0.177
Pitch excursion†	–0.053
Maximum sideslip magnitude‡	**–0.293***
Sideslip excursion‡	**–0.220**
Maximum yaw magnitude‡	–0.021
Yaw excursion‡	0.005

†Path linearity calculated from regression of *x,y*-coordinates of center of rotation (COR) in lateral-view videos.
‡Path linearity calculated from regression of *x,y*-coordinates of COR in ventral-view videos.
Limb cycles, N=96.
Bold type indicates significant relationships (P<0.05).
*Significant relationships after sequential Bonferroni correction for multiple comparisons.

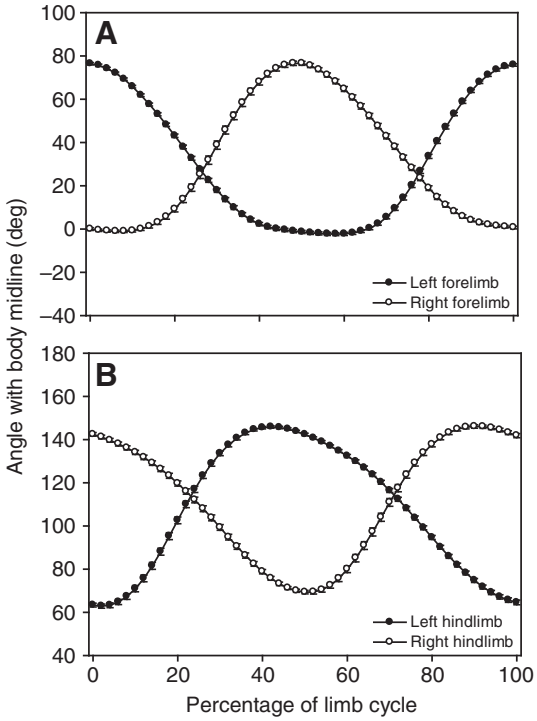

Fig. 3. Mean kinematic profiles of (A) forelimbs and (B) hindlimbs during level rectilinear swimming in painted turtles. Open symbols indicate right side of the body; closed symbols indicate left side. A decrease in the angle with midline represents limb protraction and an increase in the angle represents limb retraction. Note the synchronous movements of contralateral forelimbs and hindlimbs and the alternating movements of the ipsilateral forelimbs and hindlimbs. Note, because the maximum value for a given trial does not always occur at the same percentage of the limb cycle, it is possible that calculated maximum values may be different from the maximum values seen in mean kinematic profiles.

to protraction (recovery stroke) occurred near the beginning or end of the limb cycle for the right hindlimb, and near the middle of the limb cycle for the right forelimb and left hindlimb. Because of the bimodal distribution of the retraction–protraction transition for the right hindlimb, additional data on the timing of limb kinematics were calculated based on the left and right forelimbs and the left hindlimb only. Based on the timing at which each limb switched from retraction to protraction, the left and right forelimbs differed by between 38 and 61% of the limb cycle (48±1%; N=96 for all kinematic data), whereas the difference in timing between contralateral forelimbs and hindlimbs ranged from –8 to 23% of the limb cycle (7±1%). In general, the forelimb began to protract following the initiation of protraction by the contralateral hindlimb (positive values); however, occasionally the forelimb began to protract before the hindlimb (negative values). The difference in timing between ipsilateral forelimbs and hindlimbs ranged from 26 to 52% (42±1%) of the limb cycle. Correlation analyses showed that none of these relative timing variables (i.e. between limb pairs) were significantly correlated with speed (P>0.05). However, differences between the timing of contralateral forelimbs and hindlimbs are significantly correlated with maximum sideslip magnitude (Pearson correlation, r=–0.276, P<0.05, N=96) and sideslip excursion (Pearson correlation, r=–0.212, P=0.038).

Body stability

Values for body stability parameters (heave, pitch, sideslip and yaw) were calculated for each of the individual 96 cycles and are presented along with results of an ANOVA testing for intraspecific differences in Table 3. Neither heave nor pitch showed a temporal pattern during the limb cycle (i.e. random and non-cyclic) and individual cycles showed a broad range of stability (Fig. 4A,B). In contrast, measures of lateral stability (sideslip and yaw) showed consistent cyclic patterns (Fig. 4C,D). At the beginning of the limb cycle, the left forelimb and right hindlimb would have just finished retracting (i.e. power stroking; Fig. 3), and because the right hindfoot produces more thrust than the left forefoot (Blob et al., 2003), this power stroke motion creates a torque, rotating the turtle to the left (0–20% of limb cycle, Fig. 4D). The body reached its maximum leftward orientation near 20% of the limb cycle and then began to rotate towards the right, becoming parallel with the path of travel near 40% of the limb cycle (Fig. 4D). The turtle was oriented to the right of the path of travel from approximately 40 to 90% of the limb cycle, and reached a maximum rightward orientation near 60% of the limb cycle. Comparisons of temporal patterns of sideslip and yaw indicate there was a lag between changes in the direction in which the body was oriented and the direction in which it was traveling (Fig. 4C,D). While the turtle was oriented to the left of the path of travel (yaw), the body continued to move towards the right (sideslip). The direction of motion switched (to the left) near the time at which the body becomes parallel with the path of travel.

Correlations between the 12 body stability parameters (adjusted for multiple comparisons) showed that 18 of 66 possible relationships were significant (P<0.05; Table 4), including two of six correlations between lateral parameters and 16 of 28 correlations between vertical parameters. However, none of the 32 correlations comparing lateral and vertical parameters were found to be significant. Additionally, regression analyses identified only weak relationships between the 12 variables of body stability and swimming velocity, with R^2-values ranging from 0.001 to 0.086. Swimming velocity explained greater than 5% of variation for only three parameters: maximum heave magnitude (y=–0.006x+0.05, R^2=0.086), heave excursion (y=–0.007x+0.06, R^2=0.053), and maximum sideslip magnitude (y=0.003x+0.01, R^2=0.055). These data indicate that increased swimming speeds result in slight improvements in heave and slight detriments in sideslip.

Table 3. Descriptive statistics for stability parameters and results of nested ANOVAs testing for differences between individual painted turtles

Stability parameters	Species	Turtle 1	Turtle 2	Turtle 3	Turtle 4	$F_{3,28}$	P
Maximum heave magnitude	0.024±0.002 (0.005–0.078)	0.023±0.003 (0.005–0.052)	0.015±0.001 (0.006–0.026)	0.029±0.004 (0.005–0.068)	0.027±0.003 (0.006–0.078)	1.070	0.378
Maximum positive heave	0.017±0.002 (–0.015–0.078)	0.017±0.003 (0.000–0.044)	0.012±0.002 (–0.009–0.026)	0.017±0.004 (–0.013–0.058)	0.019±0.003 (–0.015–0.078)	0.434	0.730
Maximum negative heave	–0.017±0.002 (–0.068–0.012)	–0.015±0.003 (–0.052–0.012)	–0.012±0.002 (–0.026–0.002)	–0.020±0.005 (–0.068–0.010)	–0.018±0.003 (–0.058–0.011)	0.916	0.446
Heave excursion	0.033±0.002 (0.007–0.119)	0.032±0.004 (0.008–0.078)	0.023±0.003 (0.007–0.049)	0.037±0.006 (0.008–0.119)	0.037±0.004 (0.007–0.116)	0.701	0.559
Maximum pitch magnitude	4.149±0.204 (0.773–11.091)	3.363±0.301 (0.773–7.524)	4.870±0.357 (2.822–9.473)	4.022±0.511 (1.179–10.548)	4.409±0.384 (1.423–11.091)	2.210	0.109
Maximum positive pitch	2.095±0.290 (–4.185–11.091)	1.333±0.436 (–2.871–5.289)	2.839±0.796 (–2.386–9.473)	2.309±0.562 (–3.543–6.912)	2.107±0.542 (–4.185–11.091)	0.438	0.727
Maximum negative pitch	–2.287±0.276 (–10.548–5.959)	–2.581±0.362 (–7.524–0.374)	–0.553±0.794 (–6.609–4.027)	–2.806±0.591 (–10.548–2.588)	–2.690±0.452 (–9.349–5.959)	0.965	0.423
Pitch excursion	4.382±0.228 (0.591–11.073)	3.914±0.345 (1.274–7.783)	3.392±0.391 (0.793–6.693)	5.115±0.598 (0.591–11.073)	4.797±0.400 (1.683–8.981)	1.734	0.183
Maximum sideslip magnitude	0.022±0.001 (0.006–0.052)	0.018±0.002 (0.006–0.033)	0.024±0.002 (0.014–0.036)	0.030±0.002 (0.016–0.052)	0.019±0.001 (0.007–0.042)	5.183	**0.006**
Sideslip excursion	0.033±0.001 (0.005–0.076)	0.027±0.002 (0.005–0.052)	0.036±0.003 (0.013–0.061)	0.042±0.003 (0.015–0.076)	0.029±0.002 (0.011–0.062)	6.065	**0.003***
Maximum yaw magnitude	7.771±0.242 (3.078–13.069)	9.565±0.353 (7.065–13.069)	7.774±0.458 (4.282–11.767)	7.505±0.513 (3.078–11.198)	6.634±0.400 (3.652–11.340)	5.039	**0.006**
Yaw excursion	11.142±0.360 (4.285–20.302)	14.964±0.525 (9.339–20.302)	10.985±0.607 (6.144–16.778)	10.993±0.680 (6.098–16.397)	8.544±0.376 (4.285–12.875)	18.172	**<0.001***

Limb cycles: total, N=96; Turtle 1, N=24; Turtle 2, N=18; Turtle 3, N=21; Turtle 4, N=33.
Values are means ± s.e.m., with ranges indicated in parentheses.
Bold type indicates a significant difference between individuals (P<0.05).
*Significant relationships after sequential Bonferroni correction for multiple comparisons.

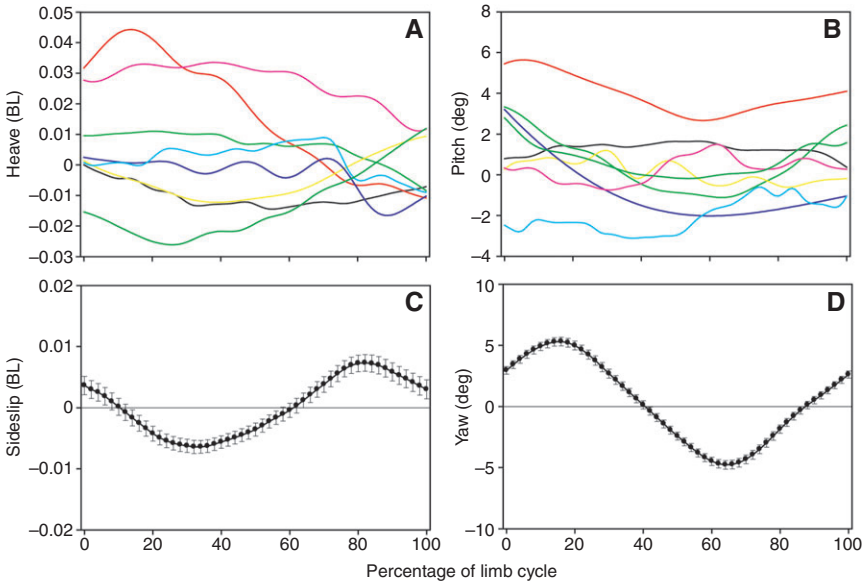

Fig. 4. Profiles of body stability during limb cycles in painted turtles. (A) Heave measured in body lengths (BL). Eight randomly selected representative trials indicating variable, non-cyclic patterns during the course of a limb cycle. Positive and negative values indicate that the lateral center of rotation (COR) is above or below the path of travel, respectively. (B) Pitch. Eight randomly selected representative trials indicating variable, non-cyclic patterns during the course of a limb cycle. Positive and negative values indicate that the turtle is pitched upward or downward relative to the path of travel, respectively. (C) Sideslip measured in body lengths. Mean profile (all trials) during limb cycle showing cyclic behavior. Symbols represent means ± s.e.m. (N=96). Positive and negative values indicate that the ventral COR is displaced to the left or right of the path of travel, respectively. (D) Yaw. Mean profile (all trials) during limb cycle showing cyclic behavior. Symbols represent means ± s.e.m. (N=96). Positive and negative values indicate that the body is yawed to the left or right of the path of travel, respectively. In addition, because the maximum value for a given trial does not always occur at the same percentage of the limb cycle, it is also possible that calculated maximum values may be different from the maximum values seen in mean kinematic profiles.

Table 4. Pearson correlations between stability parameters in painted turtles

	Maximum sideslip magnitude	Sideslip excursion	Maximum yaw magnitude	Yaw excursion	Maximum heave magnitude	Maximum positive heave	Maximum negative heave	Heave excursion	Maximum pitch magnitude	Maximum positive pitch	Maximum negative pitch
Sideslip excursion	**0.845***	–									
Maximum yaw magnitude	**0.244**	0.152	–								
Yaw excursion	0.099	0.001	**0.687***	–							
Maximum heave magnitude	0.147	0.122	–0.089	–0.066	–						
Maximum positive heave	0.108	0.132	–0.030	–0.059	**0.751***	–					
Maximum negative heave	**–0.223**	**–0.249**	0.021	–0.056	**–0.637***	–0.156	–				
Heave excursion	**0.217**	**0.250**	–0.034	–0.003	**0.914***	**0.766***	**–0.754***	–			
Maximum pitch magnitude	0.069	0.156	**–0.257**	**–0.211**	**0.518***	**0.476***	**–0.375***	**0.560***	–		
Maximum positive pitch	0.092	0.081	–0.061	–0.112	0.064	0.072	0.047	0.017	**0.276**	–	
Maximum negative pitch	0.048	–0.020	0.041	–0.005	**–0.274**	**–0.277**	0.164	**–0.291**	**–0.202**	**0.678***	–
Pitch excursion	0.059	0.127	–0.127	–0.137	**0.413***	**0.428***	–0.138	**0.374***	**0.597***	**0.452***	**–0.350***

Limb cycles, *N*=96.
Shaded area indicates correlations between lateral and vertical stability parameters.
Bold type indicates significant relationships ($P<0.05$).
*Significant relationships after sequential Bonferroni correction for multiple comparisons.

Head stability

Head stability parameters were calculated for each of the individual 96 cycles (Table 5). The vertical angle between the head and body did not show cyclic patterns during the cycle and instead was held fairly constant in the direction of the prey stimulus. The lateral angle (i.e. yaw) between the head and path of travel did show cyclic patterns, with the head and body rotating in opposite directions during the limb cycle. Yawing of the head and body produces a displacement of the anterior-most point of the head (nose point) and plastron (anterior plastron point) from the path of travel. The displacement of these points showed the same, mirrored pattern observed for the angles between the head and body and path of travel. However, although the angular deviations between both the head and body, and the path of travel, had similar magnitudes and excursions, the differences in the displacement of the nose and the anterior edge of the plastron were considerably higher, with the anterior edge of the plastron having a more stable trajectory than the nose.

Stability differences between freshwater and marine turtles

Stability parameters for painted turtles were compared with those of post-hatchlings (carapace length: 5.5–8.0 cm) from two species of marine turtles (the loggerhead, *Caretta caretta*, and green turtle, *Chelonia mydas*) that had been measured in a study using similar experimental methods and criteria for the inclusion of trials (Dougherty et al., 2010). All sea turtles pursued prey stimuli using exclusive synchronous foreflipper flapping, with mean swimming velocities during cycles of 5.5 BL s^{-1} for loggerheads and 5.4 BL s^{-1} for green turtles. Differences in sample size and results of statistical tests between analyses for sea turtles presented here and those reported previously (Dougherty et al., 2010) are because of removal of trials with outliers (>3 standard deviations from the mean), which left 120 cycles from eight individual loggerheads (two to six trials per turtle) and 72 cycles from six individual green turtles (three to five trials per turtle).

A nested ANOVA (adjusted by sequential Bonferroni) including all three species found significant species effects for seven of eight

Table 5. Head stability data for limb cycles in painted turtles

Stability parameters	Minimum	Maximum	Mean ± s.e.m.
Vertical head–body angle magnitude (deg)	2.89	31.96	15.09±0.73
Vertical head–body angle excursion (deg)	1.08	16.13	6.00±0.32
Lateral head/body angle magnitude (deg)	5.55	28.50	14.98±0.54
Lateral head/body angle excursion (deg)	9.04	34.13	18.07±0.64
Maximum head yaw magnitude (deg)	3.25	21.81	9.74±0.44
Maximum head yaw excursion (deg)	3.56	19.17	9.67±0.33
Maximum nose displacement (BL)	0.019	0.123	0.056±0.002

Limb cycles, *N*=96.
BL, body length.

stability parameters tested (Table 6), although pairwise tests indicated only one parameter (maximum heave magnitude) differed significantly between the two species of marine turtle (Fig. 5A). No significant differences were detected between the three species for maximum yaw magnitude (Fig. 5G). Painted turtles displayed the highest yaw excursion of the three species, although they only differed significantly from green turtles (Fig. 5H). For the six remaining parameters, painted turtles displayed significantly greater stability than either of the species of marine turtle (Fig. 5A–F).

DISCUSSION

Characteristics of aquatic stability in swimming freshwater turtles

During rectilinear swimming, painted turtles use asynchronous movements of contralateral forelimb and hindlimb pairs. With this locomotor mode, maximum stability would be expected if the two contralateral limb pairs stay completely out of phase (i.e. movements differing by 50% of the limb cycle). Our results showed that the mean difference in timing between the start of protraction for the two contralateral pairs was 48% of the limb cycle. The timing of protraction for the two limbs within each contralateral pair was also tightly matched, differing by a mean of only 7% of the limb cycle. Differences in the timing of motion between contralateral forelimbs and hindlimbs was significantly correlated with maximum sideslip magnitude and sideslip excursion, highlighting the importance of maintaining proper phase relationships between the appendages for maintaining stability (Wiktorowicz et al., 2007).

Parameters of vertical stability (heave and pitch) are non-cyclic in painted turtles with high variability from cycle to cycle. In contrast, measures of lateral stability (sideslip and yaw) show highly repeatable cyclic patterns. Following retraction of a contralateral forelimb and hindlimb pair, the body rotates (i.e. yaws) away from the side of the retracting hindlimb. This happens because the hindfeet have more webbing than the forefeet and, therefore, hindfeet act as larger paddles and are able to produce more thrust (Blob et al., 2003). The lag in timing between changes in yaw direction and changes in sideslip motion are the result of momentum that continues carrying the body in one direction for a short period even after the body has been reoriented toward the opposite direction.

The vertical angle of the head was held fairly constant during a cycle, whereas the lateral angle of the head followed a cyclic pattern, yawing in the opposite direction of the body. The yawing motion of the head is probably due to hydrodynamic resistance as the body rotates side to side; this resistance may help to reduce overall body yaw. An examination of the motion of the head relative to the path of travel showed that the head yawed to a similar magnitude as the body. However, the resulting lateral displacement of the anterior points of the head (nose) and the plastron show that displacement of the nose is greater (i.e. the head is less stable) than the anterior plastron point.

Comparison of stability between freshwater and marine turtles

A major focus of this study was to compare parameters of hydrodynamic stability between turtles using different modes of propulsion [freshwater *vs* marine turtles, with data for the latter from Dougherty et al. (Dougherty et al., 2010)]. In particular, we tested three hypotheses of how different modes of propulsion can produce differences in stability. Our first prediction stated that because the primary direction of motion for the limbs of freshwater turtles is front to back, they were expected to have lower levels of heave than marine turtles. Consistent with our predictions, for heave magnitude and excursion values were significantly smaller (approximately half) for painted turtles than the two species of marine turtle (Fig. 5A,B). Our second prediction stated that because marine turtles swim using limbs at only the anterior end of the body, they would encounter higher levels of pitch than freshwater turtles. Consistent with our predictions, for pitch magnitude and excursion, painted turtles had significantly lower values than the two marine turtles (Fig. 5C,D). Our third prediction stated that because limb motions occur at the same time on both sides of the body, marine turtles would have lower levels of sideslip and yaw. However, results for three of our four lateral stability parameters were not consistent with our predictions (Fig. 5E–H). Although painted turtles did have significantly greater yaw excursion than one of the marine species (green turtles), they had significantly lower values of maximum sideslip magnitude and excursion compared with both marine species (Fig. 5E,F). In addition, no significant differences were detected between the species for maximum yaw magnitude.

Despite the perceived advantages of synchronous forelimb movement, painted turtles are, on average, more stable than marine turtles with respect to parameters of sideslip (Fig. 5E,F). Although marine turtles are capable of similarly small sideslip motions (Fig. 5E,F), this probably only occurs when both forelimbs move with precisely synchronized speed and orientation. In comparison, the alternating limb kinematics of freshwater turtles actually may be crucial to their lower levels of sideslip. Although the power strokes

Table 6. Results of mixed-model nested ANOVA testing for interspecific differences in stability parameters among turtle species

	Species			Individual			Trial		
Stability parameters	*F*	*P*	d.f.	*F*	*P*	d.f.	*F*	*P*	d.f.
Maximum heave magnitude	31.69	**<0.001***	2,14.41	1.96	0.029	15,78	3.10	<0.001	78,192
Heave excursion	38.45	**<0.001***	2,14.42	2.01	0.025	15,78	1.64	0.003	78,192
Maximum pitch magnitude	29.91	**<0.001***	2,14.10	1.27	0.239	15,78	1.76	<0.001	78,192
Pitch excursion	11.90	**<0.001***	2,14.56	2.65	0.003	15,78	1.38	0.039	78,192
Maximum sideslip magnitude	30.72	**<0.001***	2,14.24	1.52	0.119	15,78	3.79	<0.001	78,192
Sideslip excursion	23.98	**<0.001***	2,14.44	2.06	0.021	15,78	1.43	0.025	78,192
Maximum yaw magnitude	1.60	0.235	2,14.53	2.47	0.005	15,78	1.06	0.369	78,192
Yaw excursion	6.48	**0.010***	2,14.77	4.98	<0.001	15,78	1.33	0.061	78,192

Limb cycles: *Chrysemys picta*, *N*=96; *Caretta caretta*, *N*=120; *Chelonia mydas*, *N*=72.
Bold type indicates significant differences for main effect ($P<0.05$).
*Significant relationships for main effect (species) after sequential Bonferroni correction for multiple comparisons.
Test of main effect corrected for unbalanced design; adjusted d.f. are reported.
See Materials and methods for detailed description of ANOVA design.

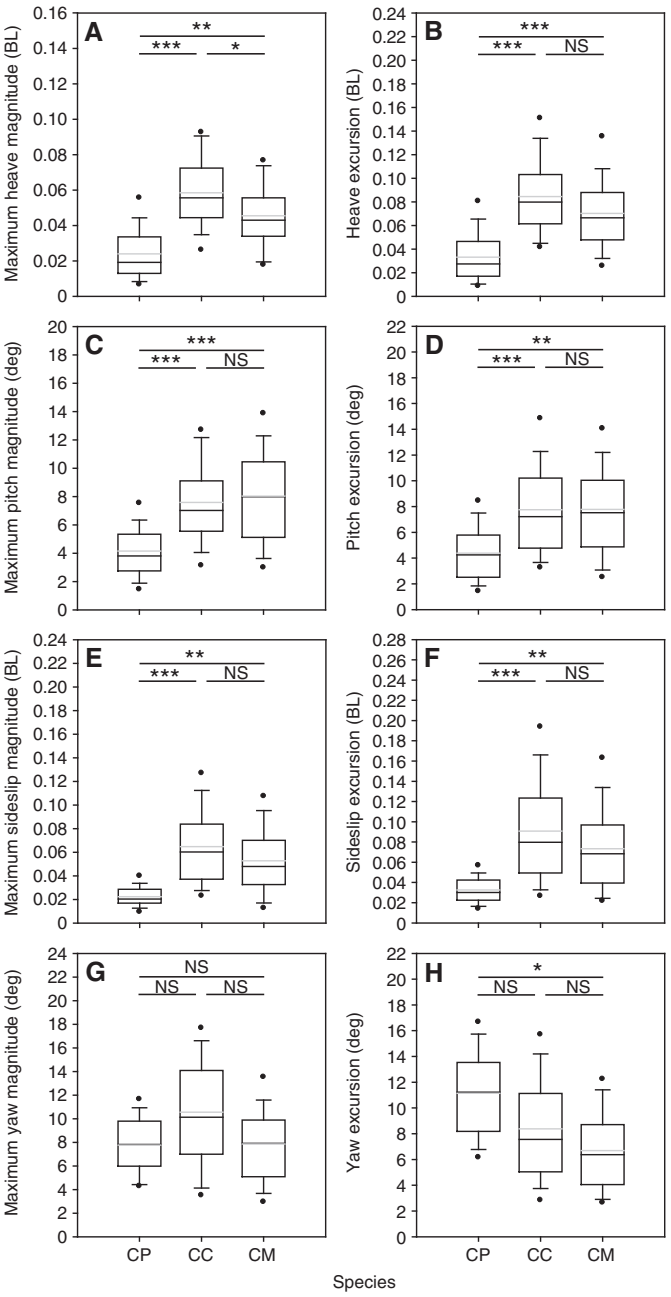

Fig. 5. Box-plots comparing values of body stability for eight focal parameters with results of pair-wise nested ANOVAs. Painted turtles (CP; N=96), loggerhead turtles (CC; N=120) and green turtles (CM; N=72). Boxes enclose the median (centerline) and the 25th and 75th percentiles (bottom and top of boxes, respectively). Whiskers indicate the 10th and 90th percentiles; circles indicate the 5th and 95th percentiles. Light gray lines indicate the mean. Significance levels: *P<0.05, **P<0.01, ***P<0.001; NS, not significant. Endpoints of horizontal lines indicate species used in each test. Sequential Bonferroni correction did not alter significance of pair-wise comparisons.

of contralateral forelimbs and hindlimbs produce displacements away from the path of travel, if properly phased, the alternating movements of the two contralateral limb pairs shift the COR back toward the path of travel, thus limiting extreme values. Other studies have also noted the importance of phased locomotor movements in increasing stability (Hove et al., 2001; Fish et al., 2003; Wiktorowicz et al., 2007). The same mechanism is also true for body orientation (i.e. yaw). Although marine turtles are capable of smaller yaw recoil than painted turtles (Fig. 5G,H), they lack the phased limb motions that shift the anterior edge of the shell back toward the path of travel. As a result, compared with painted turtles, when a sea turtle deviates from its trajectory (i.e. yaw or sideslip) there is greater potential for high values.

It is also interesting that although painted turtles had a significantly larger yaw excursion compared with green turtles, there was no significant difference between the three species for maximum yaw magnitude (Fig. 5G). In contrast, for the other three recoil motions (heave, pitch and sideslip), patterns for parameter magnitudes mirror those for excursions. The discrepancy in this pattern for yaw occurs because although marine turtles may attain large yaw values in one direction (i.e. yaw magnitude), they do not typically also then rotate to the other side during the same limb cycle (Dougherty et al., 2010). In contrast, painted turtles always rotate to both sides during a limb cycle, so even if the maximum magnitude to one side is the same as that seen in a sea turtle, freshwater turtles will have larger excursion values because of their rotation to the other side. Sea turtles, in contrast, would exhibit analogous patterns with respect to oscillations in pitch (Dougherty et al., 2010). Marine turtles can also swim in a straight line even if their bodies are not pointing in the exact direction that they are traveling. Because they can maintain such a yaw angle (up to approximately 20 deg) (Dougherty et al., 2010) throughout a swimming sequence, sea turtles have the ability to produce a cycle with a yaw excursion that is smaller than the yaw magnitude.

Conclusions and broader comparisons

Our study provides the first quantification of stability during swimming in freshwater turtles. Using these data we were able to test the effects on stability of the two general modes of propulsion used by aquatic turtles: asynchronous rowing *vs* synchronous flapping (i.e. aquatic flight). Our results indicate that the derived propulsive mode of aquatic flight does not appear to provide enhanced stabilization relative to asynchronous rowing in turtles. These findings suggest that for small sea turtles, selection favors increased swimming speed over stability, although energetic savings associated with increased stability in sea turtles may be more evident among larger animals than those we studied.

The stability of both rowing and flapping turtle species appears lower than that of other rigid-bodied taxa. For example, across the range of speeds at which they were sampled (Fig. 6), tetradontiform fishes (boxfish and pufferfish) have lower levels of pitch and yaw than turtles, with boxfish showing translational recoil motions virtually undetectable above noise levels (Hove et al., 2001). The coordinated movement of multiple fins, large body depth that partitions flows, and prominent lateral and dorsal keels (Bartol et al., 2005; Bartol et al., 2003; Bartol et al., 2002; Bartol et al., 2008; Gordon et al., 2000; Hove et al., 2001) help boxfish to maintain such high levels of stability. In contrast, the dorsoventrally flattened bodies, more rounded dorsal profiles, extension of the neck from the body and the position of the limbs (all four located near and approximately equidistant from the COR and within the same horizontal plane) in turtles may contribute to their lower stability, but potentially enhance maneuverability (Rivera et al., 2006). Beyond the species we have examined, turtles exhibit considerable morphological diversity for which effects on stability remain untested. Studies addressing these topics will increase our understanding of the relationship between propulsive mode, body morphology and hydrodynamic stability in vertebrates, and may provide insight into the evolution of the unique morphologies found in remarkable lineages like the turtles.

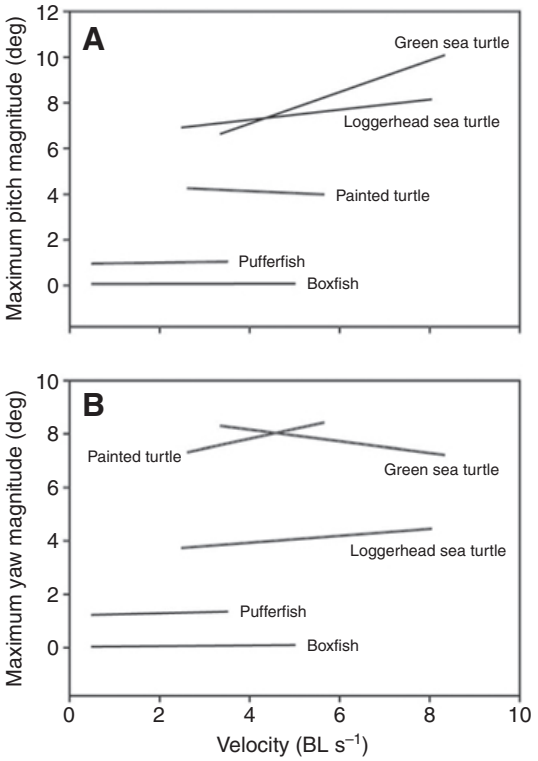

Fig. 6. Relationship between swimming velocity and (A) pitch, and (B) yaw for five species of rigid-bodied vertebrates. Lines are regression lines; ranges of lines along the *x*-axis depict the swimming speeds at which data were collected for the respective studies. Pitch: painted turtle, $y=-0.089x+4.49$ (this study); loggerhead turtle, $y=0.223x+6.358$ (Dougherty et al., 2010); green turtle, $y=0.694x+4.31$ (Dougherty et al., 2010); boxfish, $y=0.004x+0.062$ (Hove et al., 2001); pufferfish, $y=0.03x+0.94$ (Wiktorowicz et al., 2007). Yaw: painted turtle, $y=0.365x+6.36$; loggerhead turtle, $y=0.130x+3.41$ (Dougherty et al., 2010); green turtle, $y=-0.218x+9.03$ (Dougherty et al., 2010); boxfish, $y=0.013x+0.034$ (Hove et al., 2001); pufferfish, $y=0.04x+1.21$ (Wiktorowicz et al., 2007).

ACKNOWLEDGEMENTS

We thank E. Dougherty and J. Wyneken for their contributions to this project. We also thank I. Bartol, M. Ptacek, M. Childress and two anonymous reviewers for helpful comments that improved an earlier draft of this paper. N. Bennett assisted with preliminary data collection related to this work. This work was supported by NSF IOS-0517340 to R.W.B., NIH 2 R01 DC005063-06A1 to E. Peterson, Ohio University (sub-award UT10853 to R.W.B.), an ASIH Gaige Award to G.R., an American Museum of Natural History Theodore Roosevelt Memorial Award to G.R., a Society for Integrative and Comparative Biology Grant-in-Aid-of-Research to G.R. and the Clemson University Department of Biological Sciences. Deposited in PMC for release after 12 months.

REFERENCES

Aresco, M. J. and Dobie, J. L. (2000). Variation in shell arching and sexual size dimorphism of river cooters, *Pseudemys concinna*, from two river systems in Alabama. *J. Herpetol.* **34**, 313-317.
Avens, L., Wang, J. H., Johnsen, S., Dukes, P. and Lohmann, K. J. (2003). Responses of hatchling sea turtles to rotational displacements. *J. Exp. Mar. Biol. Ecol.* **288**, 111-124.
Bainbridge, R. (1963). Caudal fin and body movement in the propulsion of some fish. *J. Exp. Biol.* **40**, 23-56.
Bartol, I. K., Gordon, M. S., Gharib, M., Hove, J. R., Webb, P. W. and Weihs, D. (2002). Flow patterns around the carapaces of rigid-bodied, multi-propulsor boxfishes (Teleostei: Ostraciidae). *Integr. Comp. Biol.* **42**, 971-980.
Bartol, I. K., Gharib, M., Weihs, D., Webb, P. W., Hove, J. R. and Gordon, M. S. (2003). Hydrodynamic stability of swimming in ostraciid fishes: role of the carapace in the smooth trunkfish *Lactophrys triqueter* (Teleostei: Ostraciidae). *J. Exp. Biol.* **206**, 725-744.
Bartol, I. K., Gharib, M., Webb, P. W., Weihs, D. and Gordon, M. S. (2005). Body-induced vortical flows: a common mechanism for self-corrective trimming control in boxfishes. *J. Exp. Biol.* **208**, 327-344.
Bartol, I. K., Gordon, M. S., Webb, P. W., Weihs, D. and Gharib, M. (2008). Evidence of self-correcting spiral flows in swimming boxfishes. *Bioinspir. Biomim.* **3**, issue 1, article no. 014001.
Blob, R. W., Willey, J. S. and Lauder, G. V. (2003). Swimming in painted turtles: particle image velocimetry reveals different propulsive roles for the forelimb and hindlimb. *Integr. Comp. Biol.* **43**, 985.
Blob, R. W., Rivera, A. R. V. and Westneat, M. W. (2008). Hindlimb function in turtle locomotion: limb movements and muscular activation across taxa, environment, and ontogeny. In *Biology of Turtles* (ed. J. Wyneken, M. H. Godfrey and V. Bels), pp. 139-162. Boca Raton, FL: CRC Press.
Claude, J., Paradis, E., Tong, H. and Auffray, J.-C. (2003). A geometric morphometric assessment of the effects of environment and cladogenesis on the evolution of the turtle shell. *Biol. J. Linn. Soc. Lond.* **79**, 485-501.
Davenport, J., Munks, S. A. and Oxford, P. J. (1984). A comparison of the swimming of marine and freshwater turtles. *Proc. R. Soc. Lond. B* **220**, 447-475.
Dougherty, E. E., Rivera, G., Blob, R. W. and Wyneken, J. (2010). Hydrodynamic stability in posthatchling loggerhead (*Caretta caretta*) and green (*Chelonia mydas*) sea turtles. *Zoology* **113**, 158-167.
Fish, F. E., Peacock, J. E. and Rohr, J. J. (2003). Stabilization mechanism in swimming odontocete cetaceans by phased movements. *Mar. Mammal Sci.* **19**, 515-528.
Gillis, G. B. and Blob, R. W. (2001). How muscles accommodate movement in different physical environments: aquatic vs. terrestrial locomotion in vertebrates. *Comp. Biochem. Physiol.* **131A**, 61-75.
Gordon, M. S., Hove, J. R., Webb, P. W. and Weihs, D. (2000). Boxfishes as unusually well-controlled autonomous underwater vehicles. *Physiol. Biochem. Zool.* **73**, 663-671.
Hedrick, T. L. (2008). Software techniques for two- and three-dimensional kinematic measurements of biological and biomimetic systems. *Bioinspir. Biomim.* **3**, 034001.
Heithaus, M. R., Frid, A. and Dill, L. M. (2002). Shark-inflicted injury frequencies, escape ability, and habitat use of green and loggerhead turtles. *Mar. Biol.* **140**, 229-236.
Holm, S. (1979). A simple sequentially rejective multiple test procedure. *Scand. J. Stat.* **6**, 65-70.
Hove, J. R., O'Bryan, L. M., Gordon, M. S., Webb, P. W. and Weihs, D. (2001). Boxfishes (Teleostei: Ostraciidae) as a model system for fishes swimming with many fins: kinematics. *J. Exp. Biol.* **204**, 1459-1471.
Joyce, W. G. and Gauthier, J. A. (2004). Palaeoecology of Triassic stem turtles sheds new light on turtle origins. *Proc. R. Soc. Lond. B* **271**, 1-5.
Lighthill, J. (1975). *Mathematical Biofluiddynamics*. Philadelphia, PA: Society for Industrial and Applied Mathematics.
Lighthill, J. (1977). Mathematical theories of fish swimming. In *Fisheries Mathematics* (ed. J. H. Steele), pp. 131-144. London: Academic Press.
Long, J. H. (2006). Four flippers or two? Tetrapodal swimming with an aquatic robot. *Bioinspir. Biomim.* **1**, 20-29.
Lubcke, G. M. and Wilson, D. S. (2007). Variation in shell morphology of the western pond turtle (*Actinemys marmorata* Baird and Girard) from three aquatic habitats in northern California. *J. Herpetol.* **41**, 107-114.
Pace, C. M., Blob, R. W. and Westneat, M. W. (2001). Comparative kinematics of the forelimb during swimming in red-eared slider (*Trachemys scripta*) and spiny softshell (*Apalone spinifera*) turtles. *J. Exp. Biol.* **204**, 3261-3271.
Renous, S., de Lapparent de Broin, F., Depecker, M., Davenport, J. and Bels, V. (2008). Evolution of locomotion in aquatic turtles. In *Biology of Turtles* (ed. J. Wyneken, M. H. Godfrey and V. Bels), pp. 97-138. Boca Raton, FL: CRC Press.
Rice, W. R. (1989). Analyzing tables of statistical tests. *Evolution* **43**, 223-225.
Rivera, A. R. V. and Blob, R. W. (2010). Forelimb kinematics and motor patterns of the slider turtle (*Trachemys scripta*) during swimming and walking: shared and novel strategies for meeting locomotor demands of water and land. *J. Exp. Biol.* **213**, 3515-3526.
Rivera, G. (2008). Ecomorphological variation in shell shape of the freshwater turtle *Pseudemys concinna* inhabiting different aquatic flow regimes. *Integr. Comp. Biol.* **48**, 769-787.
Rivera, G. and Claude, J. (2008). Environmental media and shape asymmetry: a case study on turtle shells. *Biol. J. Linn. Soc.* **94**, 483-489.
Rivera, G., Rivera, A. R. V., Dougherty, E. E. and Blob, R. W. (2006). Aquatic turning performance of painted turtles (*Chrysemys picta*) and functional consequences of a rigid body design. *J. Exp. Biol.* **209**, 4203-4213.
Sokal, R. R. and Rohlf, F. J. (1995). *Biometry: The Principles and Practice of Statistics in Biological Research*. 3rd edn. New York: W. H. Freeman and Co.
Walker, J. A. (1998). Estimating velocities and accelerations of animal locomotion: a simulation experiment comparing numerical differentiation algorithms. *J. Exp. Biol.* **201**, 981-995.
Walker, J. A. (2000). Does a rigid body limit maneuverability? *J. Exp. Biol.* **203**, 3391-3396.
Wassersug, R. J. and von Seckendorf Hoff, K. (1985). The kinematics of swimming in anuran larvae. *J. Exp. Biol.* **119**, 1-30.
Webb, P. W. (1992). Is the high cost of body/caudal fin undulatory swimming due to increased friction drag or inertial recoil? *J. Exp. Biol.* **162**, 157-166.
Webb, P. W. (2002). Control of posture, depth, and swimming trajectories of fishes. *Integr. Comp. Biol.* **42**, 94-101.
Weihs, D. (2002). Stability versus maneuverability in aquatic locomotion. *Integr. Comp. Biol.* **42**, 127-134.
Wiktorowicz, A. M., Lauritzen, D. V. and Gordon, M. S. (2007). Powered control mechanisms contributing to dynamically stable swimming in porcupine puffers (Teleostei: *Diodon holocanthus*). *Exp. Fluids* **43**, 725-735.
Wyneken, J. (1997). Sea turtle locomotion: mechanics, behavior, and energetics. In *Biology of Sea Turtles* (ed. P. L. Lutz and J. A. Musick), pp. 165-198. Boca Raton, FL: CRC Press.
Zug, G. R. (1971). Buoyancy, locomotion, morphology of the pelvic girdle and hind limb and systematics of cryptodiran turtles. *Misc. Publ. Mus. Zool. Univ. Michigan* **142**, 1-98.